Fog and Cloudiness Monitoring Using Global Navigation Satellite System Precipitable Water Vapor

Lee Wonjong,[1] Choi Yunsoo,[1*] and Yoon Hasu[2]

[1]Department of Geoinformatics, University of Seoul, 163 Seoulsiripdae-ro, Dongdaemun-gu, Seoul 02504, Korea
[2]Department of Geodesy, National Geographic Information Institute,
92 Worldcup-ro, Yeongtong-gu, Suwon-si, Gyeonggi-do 443-772, Korea

Fog is formed when water vapor in the atmosphere condenses into miniscule floating water droplets, rendering a visibility of less than 1 km. Fog causes economic damage and poses a hazard to people owing to limited visibility. Fog forecasts depend on the judgment and experience of the forecaster, who bases the forecast on analysis results from meteorological models and satellite images. However, such forecasts are complicated by spatiotemporal changes and fine physical processes. To address this issue, a variety of fog studies have used the Global Navigation Satellite System (GNSS) tropospheric signal delay as an alternative. In this study, we monitored fog and cloudiness by analyzing precipitable water vapor (PWV) extracted from GNSS tropospheric delay. The analysis of the change in PWV during fog generation showed that it is difficult to detect fog from PWV using GNSS; more precise GNSS processing is required. However, it was found that cloudiness affects the change in PWV. In particular, the change in PWV is affected by high-level and middle-level clouds rather than low-level clouds. In other words, we conducted research to detect fog and cloudiness, but it was difficult to monitor them using PWV calculated from GNSS, although the use of GNSS to monitor the high-level and middle-level clouds generated good results. The results of this study will aid in quantitative cloudiness measurements, which at present are mostly performed through non-quantitative visual inspection. Furthermore, these results are expected to be helpful in the development of automatic observation devices for cloudiness measurements, satellite image processing, and weather forecasting.

1. Introduction

Fog is formed when water vapor in the atmosphere condenses into miniscule floating water droplets, rendering a visibility of less than 1 km (WMO: World Meteorological Organization).[1] Fog occurs over land and at sea, causing economic damage and a threat to human safety in the form of car and ship accidents; other impacts include flight cancellations and delays due to limited visibility. Clouds are formed as a result of air saturation when air is cooled to its dew

point, or when it gains sufficient moisture (usually in the form of water vapor) from an adjacent source to raise the dew point to the ambient temperature. Table 1 illustrates flight statistics from the Korea Airports Corporation, showing flight delays and cancellations caused by meteorological factors in 2020. Of the 3692 flight cancellations in 2020, 2309 were weather-related, representing 62.5%. Among these, cancellations due to fog accounted for 19.1% (442 cancellations), more than those due to snow or rain. Among 52084 flight delays, 1707 were caused by weather, representing 3.3%. Of these, delays due to fog accounted for 48.7% (895 delays).

Moreover, according to KoROAD's statistical analysis of traffic accidents in 2021, fog accounted for 0.1% (207 cases) of all accidents caused by weather conditions. Moreover, the mortality rate for accidents caused by fog was much higher than those caused by other weather conditions (Table 2).

Accurate fog forecasts can reduce human casualties and economic losses. Currently, fog forecasts depend on the judgment and experience of the forecaster, who bases the forecast on analysis results from meteorological models and satellite images. However, such forecasts for fog are complicated by spatiotemporal changes and fine physical processes. From a technical perspective, it is difficult to distinguish a low stratiform cloud from fog using satellite images, and it is not possible to detect fog at night, as fog is generally detected through visible light images. Moreover, it is difficult to predict the behavior of small water droplets, such as those in fog, in numerical models because the degree of saturation significantly varies depending on the particle size, such that growth and evaporation processes of water droplets coexist.

A number of researchers have used the Global Navigation Satellite System (GNSS) tropospheric signal delay to investigate precipitation, rainfall, and typhoons. The data calculated in GNSS are used as initial estimates in weather forecast numerical models, and many results

Table 1
Flight delays and cancellations caused by meteorological factors in 2020 (source: Korea Airports Corporation 2020).

Total No.		Arrival (number)					Departure (number)				
		Fog	Snow	Rain	Other	Total	Fog	Snow	Rain	Other	Total
Flight cancellation	2309	217	93	23	933	1166	225	96	19	803	1143
Flight delay	1707	422	80	18	410	930	473	53	6	245	777

Table 2
Traffic accidents caused by meteorological factors in 2021 (source: Korea KoROAD, 2022).

	No. of accidents		No. of deaths			No. of injuries	
	Number	Component ratio (%)	Number	Component ratio (%)	Fatality rate (%)	Number	Component ratio (%)
Total	203130	100.0	2916	100.0	1.4	291608	100.0
Clear	178913	88.1	2372	81.3	1.3	256686	88.0
Cloudy	6982	3.4	197	6.7	2.8	9777	3.3
Rain	13373	6.6	267	9.2	1.9	19505	6.7
Fog	207	0.1	22	0.8	10.6	294	0.1
Snow	1395	0.7	23	0.8	1.6	2217	0.8
Other	2260	1.1	35	1.2	1.5	3129	1.1

with high prediction accuracy have been published.[2–4] However, to date, few studies have focused on fog analysis using GNSS. Lee *et al.* assumed certain fog formation conditions to employ the Global Positioning System (GPS) for fog research.[5] To identify fog creation and dissipation processes, the GPS integrated water vapor (IWV) and observational data from weather stations (e.g., visibility, temperature, and relative humidity) were compared and fog classification was attempted. The type of fog can be classified with the change pattern of GPS IWV. It can be inferred that an increase in GPS IWV means the dominance of the advection effect, and a decrease in GPS IWV means the dominance of the condensation effect over the GPS site during fog. Moreover, the potential as a forecasting method was confirmed because GPS IWV can be used to identify changes in water vapor volume inside fog in advance, rather than relying on phenomenological visibility changes. Stoycheva and Guerova confirmed the high sensitivity of IWV for advection and radiation fog, concluding that IWV and the mixing ratio can serve as important tools for fog forecasting.[6] Stoycheva *et al.* installed GNSS at three altitudes (595, 1120, and 2290 m) in a foggy Bulgarian valley and estimated the change in air mass according to altitude using GNSS IWV and investigated the spatiotemporal characteristics of fog.[7] Furthermore, they simulated the results using a numerical forecasting model and ultimately confirmed an improvement in fog forecast ability.

In this study, the relationships between fog and both precipitable water vapor (PWV) resulting from the GNSS tropospheric delay and weather data were analyzed. The fog forecasting ability was analyzed using GNSS and, unlike in other studies, the relationship between PWV and clouds was analyzed.

2.   Research Theory and Method

2.1   Fog, cloudiness, and GNSS tropospheric delay

Fog is closely related to water vapor and can be classified into fog generated by the cooling of air or as fog generated by the evaporation of water vapor. Fog generated by the cooling of air includes radiation fog, advection fog, and up-slope fog, whereas that generated by the evaporation of water vapor includes frontal fog and steam fog. In this study, coastal fog, which has the characteristics of combined radiation and advection fog, was analyzed for Jeju Airport, located on the coast of Jeju Island, Korea. Coastal fog is generated when humid air from the sea condenses because of ground cooling after sunset.

Cloudiness is the estimated degree of cloud coverage in the sky. Generally, the sky is divided into eight parts in okta. Okta is a unit of cloud amount. A value of 0 indicates that there are no clouds; a value of 8 indicates that the sky is completely covered with clouds. Jeju Airport observes cloudiness by visual inspection, dividing clouds into three layers: low-level clouds, middle-level clouds, and high-level clouds. In general, low-level clouds are located between 0 and 2 km above the ground, middle-level clouds are between 2 and 6 km, and high-level clouds are between 6 and 12 km. The cloudiness portrayed in Fig. 1 is the sum of cloudiness values for low-, middle-, and high-level clouds.
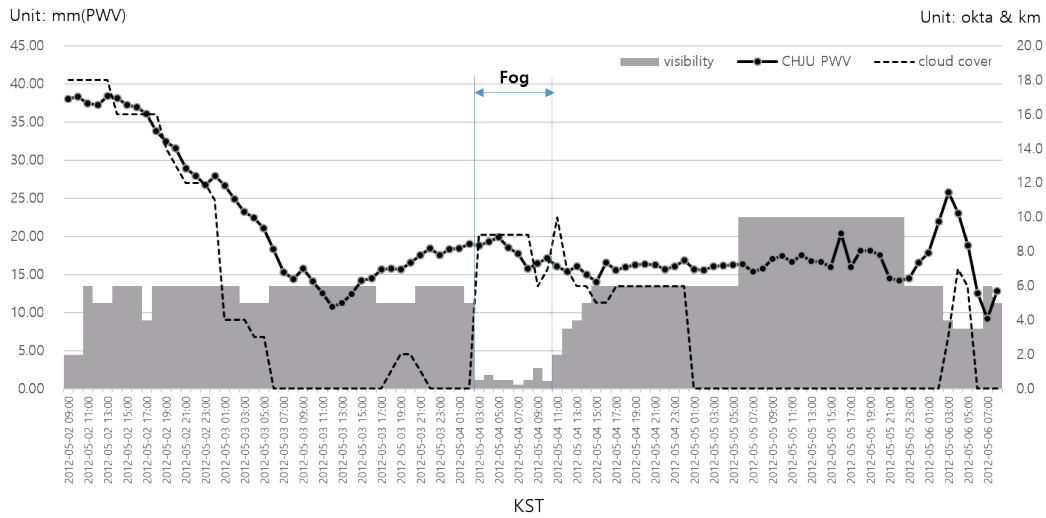
Fig. 1.   (Color online) Visibility, cloud coverage at Jeju Airport, and PWV of CHJU GNSS Station in May 2012.

The GNSS tropospheric delay signal is a phenomenon in which the GNSS signal is delayed by atmospheric constituents as it penetrates through the troposphere. This delay is considered an error factor for precise position measurement and is corrected using the tropospheric delay model at the GNSS processing stage. The analysis of the magnitude of the GNSS signal delay can provide various meteorological data such as sea level variation, snowfall, and soil water changes.[8]

The tropospheric delay can be estimated during GNSS data processing, generally as the zenith total delay (ZTD), and the PWV and IWV of the troposphere can be calculated using the estimated ZTD. The accuracies of PWV and IWV using GNSS have been considered in previous studies, and the reliabilities of GNSS PWV and IWV have been verified by comparing radiosonde or microwave radiometer (MWR) data with the amount of water vapor.[5,9–12] The theory behind GNSS tropospheric delay estimates was described in detail by Schuler[13] and is briefly presented here.

The ZTD parameter refers to a signal delay in the zenith direction of ~2 to 3 m, which can be divided into the zenith hydrostatic delay (ZHD) due to the dry gas component and the zenith wet delay (ZWD).[14] ZHD can be estimated using meteorological data or meteorological models of the point where GNSS is observed. ZWD can be calculated using the difference between ZTD and ZHD [Eq. (1)].

$$ZTD = ZHD + ZTD \tag{1}$$

ZHD with ground pressure and station altitude is calculated using Eq. (2).[15]

$$ZHD = \frac{\left(2.2779 \pm 0.0024\right)\left[\dfrac{\text{m}}{\text{hPa}}\right] P_s}{1 - 0.00266\cos 2\phi - 0.00028\left[\dfrac{1}{\text{km}}\right] h} \tag{2}$$

Here, P_s is the surface/antenna pressure (hpa), ϕ is the ellipsoidal latitude, and h is the surface/antenna height above the ellipsoid (km).

ZWD is more difficult to estimate than ZHD because the amount of water vapor varies depending on space and time. The estimation of ZWD uses the a priori method, in which ZTD can be expressed as the sum of the a priori hydrostatic delay (AHD), a priori wet delay (AWD), and zenith delay correction [ZDC; Eq. (3)]. ZDC is a correction term for the amount of a priori delay, which is estimated in GNSS data processing:[16]

$$ZTD = AHD + AWD + ZDC. \tag{3}$$

AHD is calculated using Eq. (4) and AWD is generally about 0.1 m:

$$AHD = 2.29951e^{-0.000116h}, \tag{4}$$

where h represents the altitude [km] of the ground GNSS station. Equations (1) and (3) from ZWD can be calculated using Eq. (5).

$$ZWD = \left[AHD + AWD + ZDC \right] - ZHD \tag{5}$$

ZWD can be converted to slant wet delay [SWD; Eq. (6)], PWV [Eq. (7)], and IWV [Eq. (8)].

$$SWD = m_w(\varepsilon) \cdot ZWD \tag{6}$$

$$PWV = ZWD / Q \tag{7}$$

$$IWV = \rho Q \cdot ZWD \tag{8}$$

Here, m_w is the wet mapping function, ρ is the density of water, and Q is the conversion factor. The mapping function is the relationship between the amount of delay in the zenith direction and the slant. ε represents the altitude angle between the observation point and the receiver. Q is determined using refraction constants and mean temperature equations through Eq. (9):

$$Q = \frac{10^6}{\rho R_v \left[\dfrac{k_3}{T_m} + k_2' \right]}, \tag{9}$$

where k_2' and k_3 refer to refractive index constants, R_v refers to the gas constant of water vapor, and T_m refers to a mean temperature in the troposphere. The mean temperature equation refers to the equation of mean temperature and temperature on the ground.

2.2 GNSS data processing

High-precision data processing is needed to calculate PWV accurately. In this study, the Bernese GNSS Software 5.2 developed by the University of Bern, Switzerland, was used for data processing and the precise point positioning (PPP) strategy was taken for the data processing method.[17,18] PPP provides high processing speed for GNSS stations and sufficient precision in the PWV calculation.[19] Compared with relative positioning, the processing results from PPP are not affected by reference stations.

The parameters and models used to remove various GPS errors are given in Table 3. The final product of the Center for Orbit Determination in Europe (CODE) was used for precise ephemeris, clocks, and data. Finally, Vienna Mapping Function 1 (VMF1) was used to perform data processing for mapping functions, thereby analyzing the effect of mapping function on the accuracy of data processing.[20]

3. GNSS Tropospheric Delay Analysis

3.1 Research area and processing period

Jeju Airport was chosen as the research area owing to its foggy environment, which reflects its coastal location. In addition, abundant weather data for the location are available. Finally, the verification of weather data by comparison with data collected by the Jeju Meteorological Office is possible. The time range was set from 2012 to 2016, when continuous GNSS data can be secured owing to changes in the GNSS receiver, setting errors, and so forth. Fog was analyzed using GNSS data from the Jeju GNSS regular observatory of the National Geographic Information Institute installed at the Jeju Meteorological Office and GNSS data from the Jeju Tide Station of the Korea Hydrographic and Oceanographic Agency, which is installed at the 7th pier of Jeju. The straight-line distance between the Jeju Meteorological Office and the Jeju Tide Station is 0.5 km, allowing for the verification of the GNSS tropospheric delay results. The straight-line distance between Jeju Airport and the Jeju Meteorological Office is approximately 3 km, and Jeju Airport and the tide station are approximately 3.5 km apart (Fig. 2). Table 4 shows the latitude and longitude coordinates of Jeju Airport, the Jeju Meteorological Office, and the Jeju Tide Station.

Table 3
GNSS data processing configuration.

Processing engine	Bernese 5.2
Data processing strategy	PPP
Satellite ephemeris/clocks	CODE Final
Ionosphere file (ION)	CODE ION
Reference frame (coordinate, velocity)	IGS2014
A priori troposphere/mapping function model	Vienna Mapping Function 1 (VMF1)
ZTD parameter sampling time	Hourly
Ocean tide loading model (BLQ)	FES 2004
Phase center variation (PCV)	PCV_COD.I14
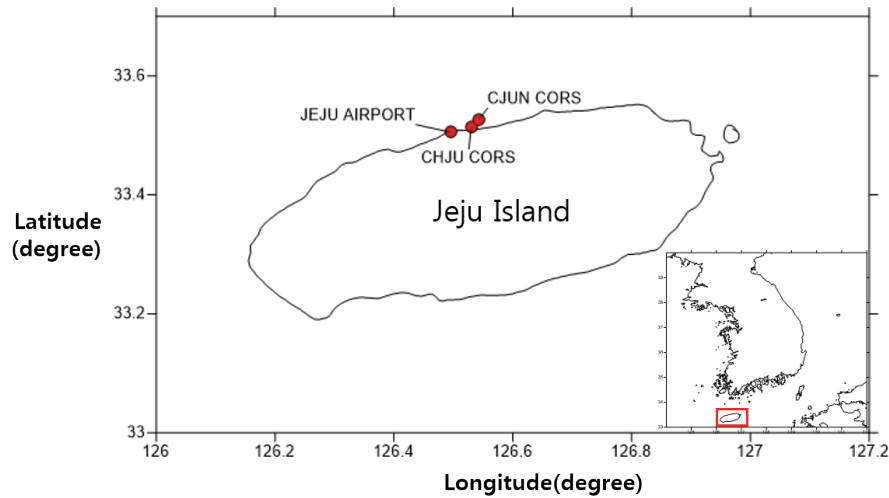
Fig. 2.　　(Color online) Map of research area (Jeju Island, Korea).

Table 4
GNSS data processing configuration.

Site	Latitude (deg)	Longitude (deg)
Jeju Airport	33.5056	126.4950
Jeju Korea Meteorological Office (CHJU)	33.5138	126.5298
Jeju Tide Station (CJUN)	33.5275	126.5431

Weather data at Jeju Airport were collected for a five-year period, from 2012 to 2016. Fog was defined as a visibility of less than 1 km and no rain. A total of 20 cases of fog were selected, namely, four in 2012, five in 2013, four in 2014, four in 2015, and three in 2016. GNSS processing was performed for the same period.

Figures 3 and 4 show the weather data from Jeju Airport and the Jeju Meteorological Office for three days of each month in January, April, August, and December 2012. Temperatures and pressures were found to be similar. Temperature and pressure are important elements for converting tropospheric delay results into PWV, and various meteorological elements (e.g., cloud amount and visibility) can be used, even if acquired at two different locations. For example, the weather data from Jeju Airport contain a lot of data related to clouds, whereas those from the Jeju Meteorological Office can provide detailed information about conditions on the ground.

3.2　Relationship between fog and GNSS PWV

The relationship between fog and the GNSS tropospheric signal delay was analyzed using PWV. PWV, which quantifies water vapor amount in the atmosphere, was obtained by converting the vapor amount included in the atmosphere into the vertical depth (mm) of the air column as a function of unit area.[21] In contrast with radiosondes and MWRs, PWV using GNSS is independent of the observation time and weather situation; it is also cost-effective. Previous studies have compared PWV using GNSS with that using radiosondes or MWRs and found that they deliver similar results.[2–7] The accuracy of PWV is affected by those of
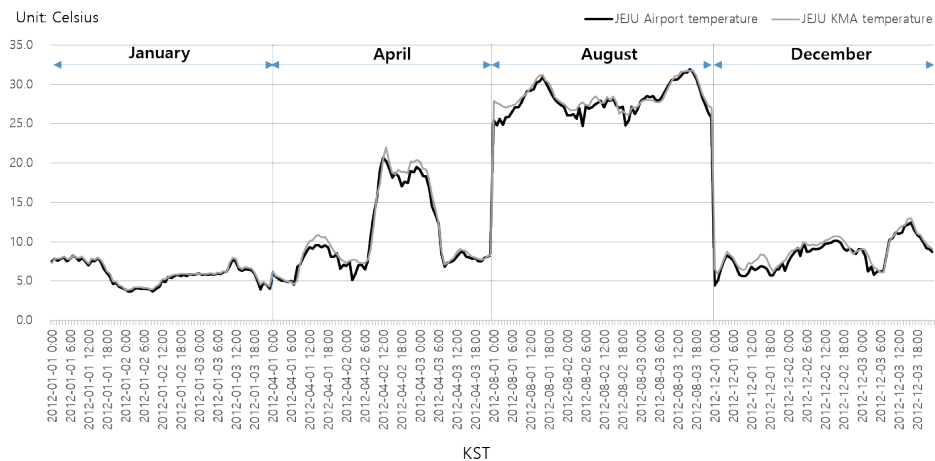
Fig. 3.   (Color online) Temperature data for Jeju Airport (black line) and Jeju Korea Meteorological Office (gray line) from 01 Jan 2012 to 31 Dec 2012.
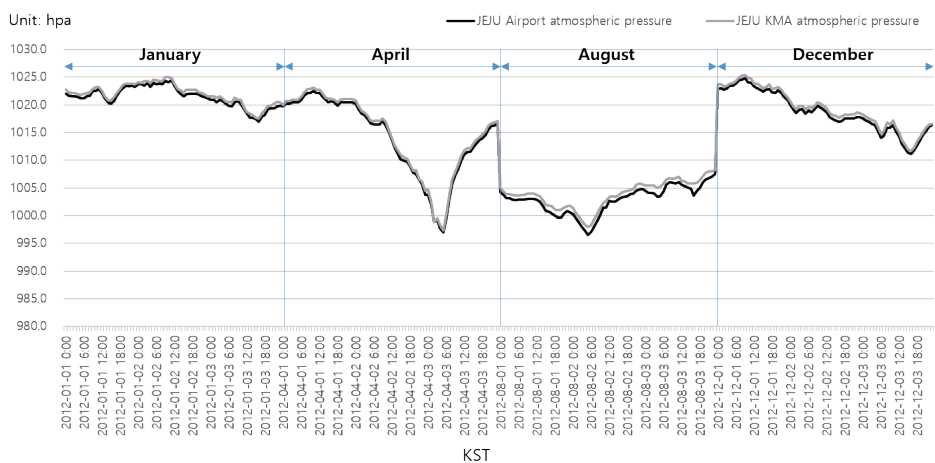
Fig. 4.   (Color online) Pressure data for Jeju Airport (black line) and Jeju Korea Meteorological Office (gray line) from 01 Jan 2012 to 31 Dec 2012.

temperature and pressure, and the data from the Jeju Meteorological Office, where GNSS is installed, were used to determine these parameters.

3.2.1   CASE 1: Fog analysis on 4 May 2012

The ZTD of the GNSS installed at the Jeju Meteorological Office and that at the Jeju Tide Station are compared, and the ZTD shows similar results as shown in Fig. 5. Figure 6 shows visibility, temperature, and humidity on 4 May 2012. Fog is caused by a decrease in temperature and an increase in humidity. On this day, fog occurred from 2:00 to 10:00.

The change in PWV during this period is shown in Fig 1. PWV increased prior to fog formation and decreased after fog dissipation. This phenomenon is similar to the case described
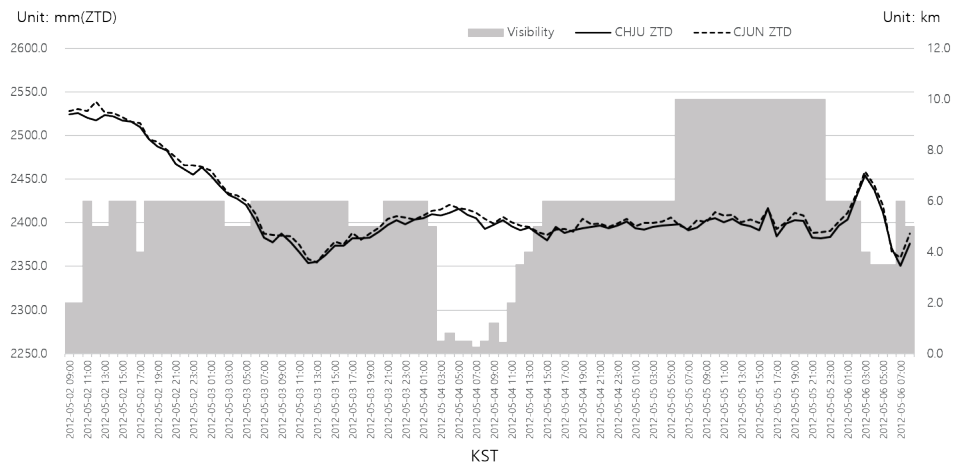
Fig. 5.   GNSS ZTD of Jeju Meteorological Office (CHJU GNSS station; black lines) and Jeju Tide Station (CJUN GNSS station; grey dotted line) from 02 May 2012 to 06 May 2012.
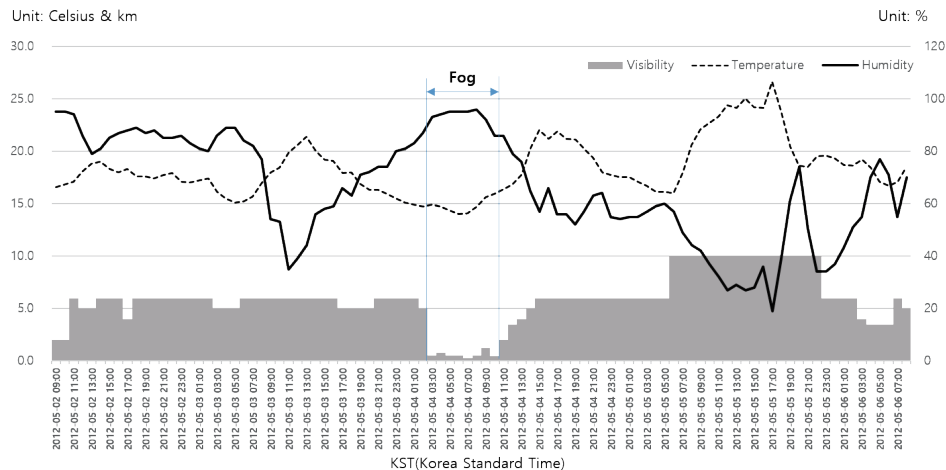
Fig. 6.   (Color online) Visibility, temperature, and humidity at Jeju Airport in May 2012.

by Lee *et al.*,[5] where the water vapor amount increased as advection fog was generated. Interestingly, there was a high correlation between cloudiness and the change in *PWV*, as illustrated by Fig. 1. The correlation between the two elements was calculated to be 0.839.

On 2 May 2012, a large change in PWV was detected; this change was affected by rainfall. From 1:00 to 6:00 on 6 May, the change in PWV was larger than that for fog generation. There was no rainfall at that time, and the observed cloudiness and PWV increased. To analyze the cause, cloudiness was expressed according to cloud level, as shown in Fig. 7, and was found to be caused by middle-level clouds. Although the PWV could have increased as a result of a concurrent increase in humidity, this is unlikely as the change in PWV was not significant during a large change in humidity between 19:00 and 21:00 on 5 May. As shown in Fig. 7, there were also cases when the cloudiness of low-level clouds exceeded 8 during the fog period. This indicates that the sky was completely covered by other meteorological phenomena, such as fog.[22]
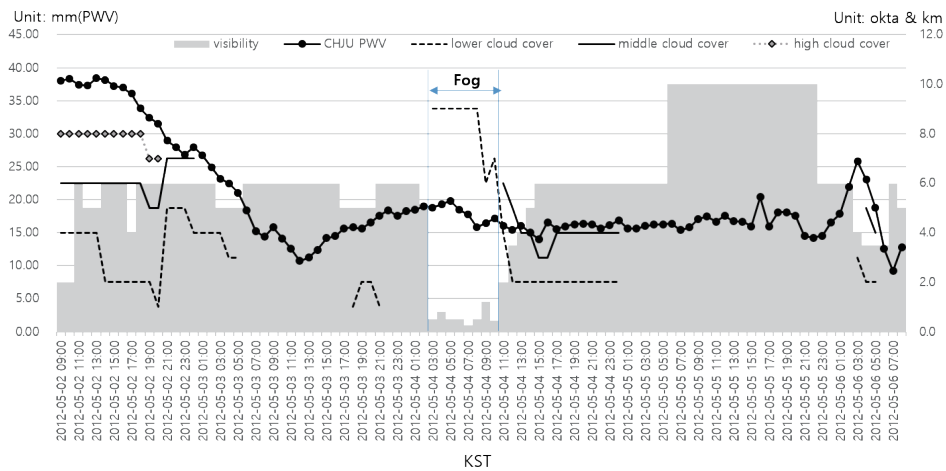
Fig. 7.   (Color online) Visibility and cloud coverage for different altitudes at Jeju Airport, and PWV of CHJU GNSS Station in May 2012.

3.2.2   CASE 2: Fog analysis on 7 March 2013

In 2013, fog occurred for 4 h from 22:00 on 7 March to 1:00 on 8 March. Figure 8 shows the temperature and humidity of the corresponding period, with fog features coincident with lower temperature, higher humidity, no rain, and a visibility of less than 1 km.

Figure 9 shows the *PWV* of the Jeju Meteorological Office GNSS station and the visibility and cloudiness of Jeju Airport. As in Case 1, the correlation between cloudiness and *PWV* was very high. Case 2 shows that *PWV* decreases before fog occurs and increases after fog is over. This is similar to the *PWV* variation of radiation fog shown by Lee *et al.*[23]

Figure 10 shows the cloudiness according to altitude. The *PWV* increased owing to the effect of middle-level cloudiness. When fog occurs, low-level cloudiness increases, but changes in *PWV*, which are related to the amount of water vapor, appear small.

3.2.3   CASE 3: Fog analysis on 22 May 2014

Figure 11 shows the temperature and humidity of fog that occurred on 22 May 2014, with the fog due to a temperature decrease and a humidity increase. As shown in Fig. 12, it rained on the morning of 20 May; at this time, the change in *PWV* was large and the correlation with cloudiness was high. During the fog period, the cloudiness increased, but the change in *PWV* was small. Figure 13 shows the cloudiness according to altitude. During the fog period, low-level cloudiness was greatly increased, but the change in *PWV* was not significant.

3.2.4   CASE 4: Fog analysis on 15–17 July 2015

Figure 14 shows the temperature and humidity of fog that occured in July 2015; high temperature and humidity were maintained owing to the summer season. Fog occurred briefly for just 1–2 h. Figure 15 shows the *PWV*, visibility, and total cloudiness for the same period.
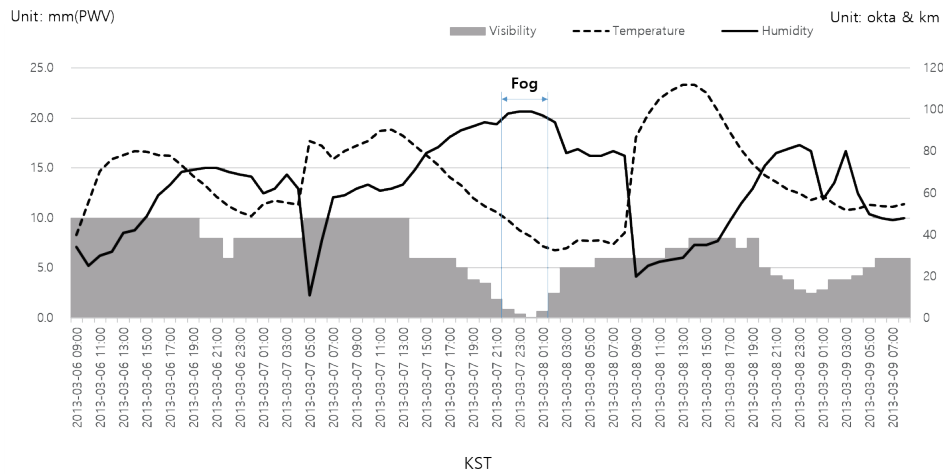
Fig. 8.   (Color online) Visibility, temperature, and humidity at Jeju Airport in March 2013.
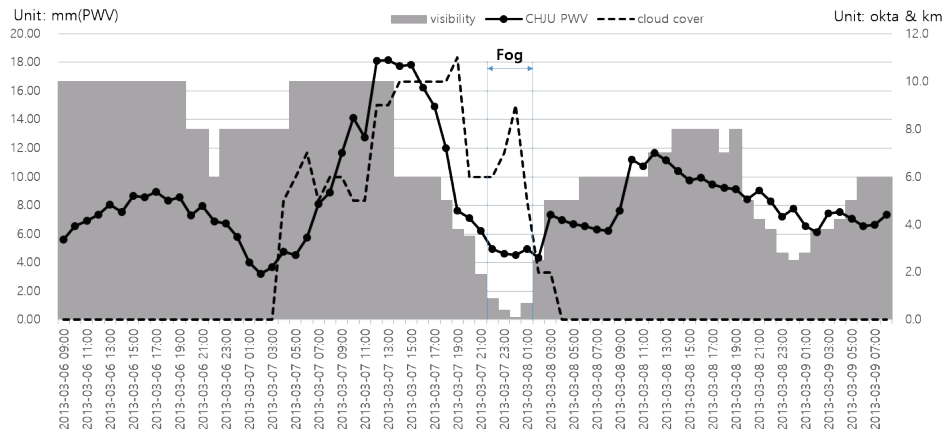
Fig. 9.   (Color online) Visibility, cloud coverage at Jeju Airport, and PWV of CHJU GNSS Station in March 2013.
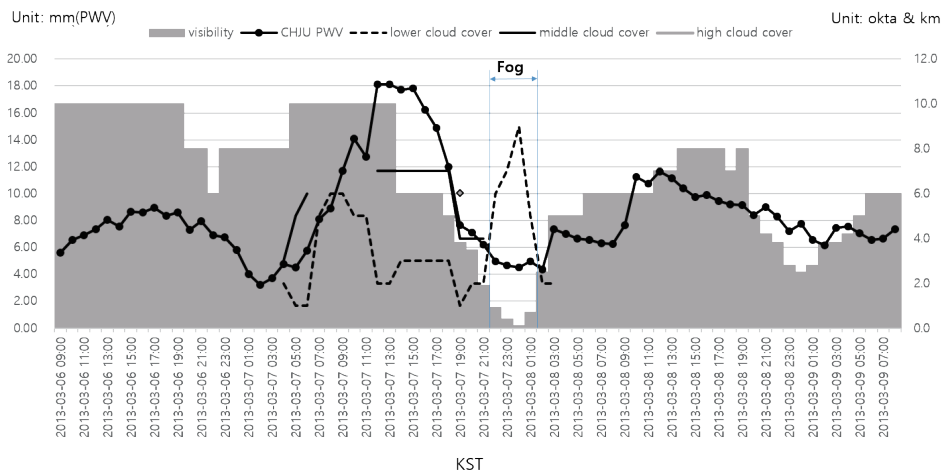
Fig. 10. (Color online) Visibility and cloud coverage for different altitudes at Jeju Airport, and PWV of CHJU GNSS Station in March 2013.
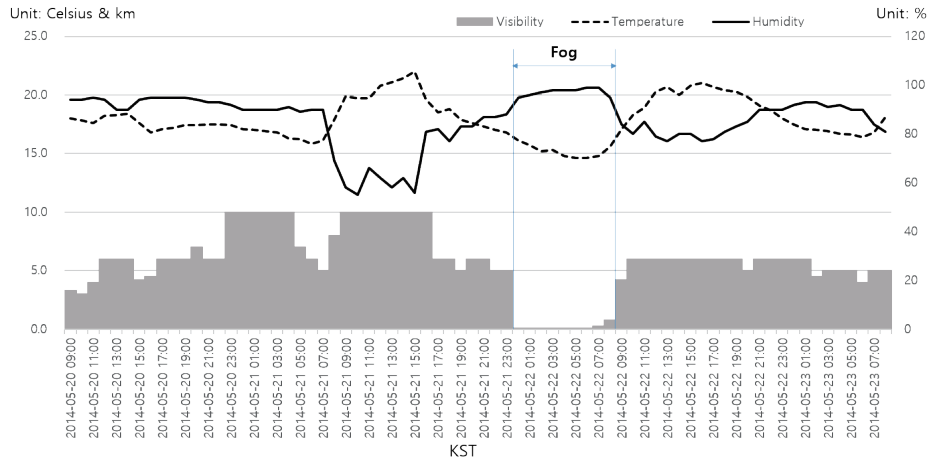
Fig. 11.   (Color online) Visibility, temperature, and humidity at Jeju Airport in May 2014.
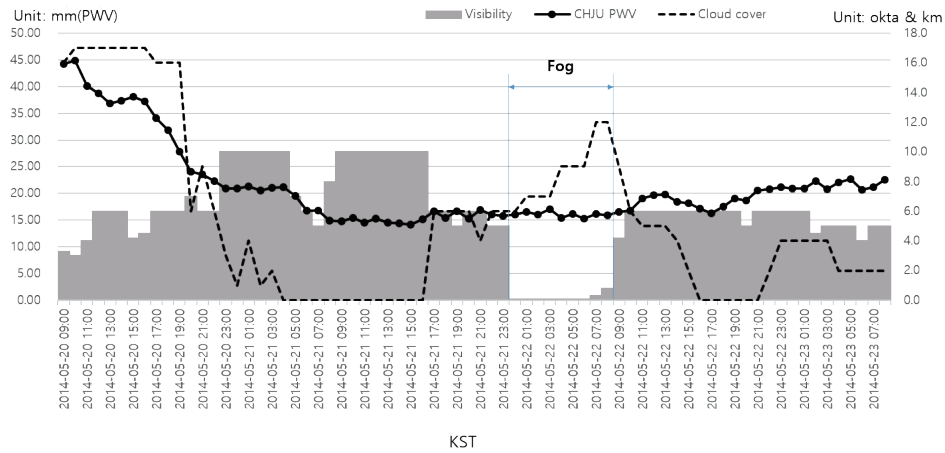
Fig. 12.   (Color online) Visibility, cloud coverage at Jeju Airport, and PWV of CHJU GNSS Station in May 2014.
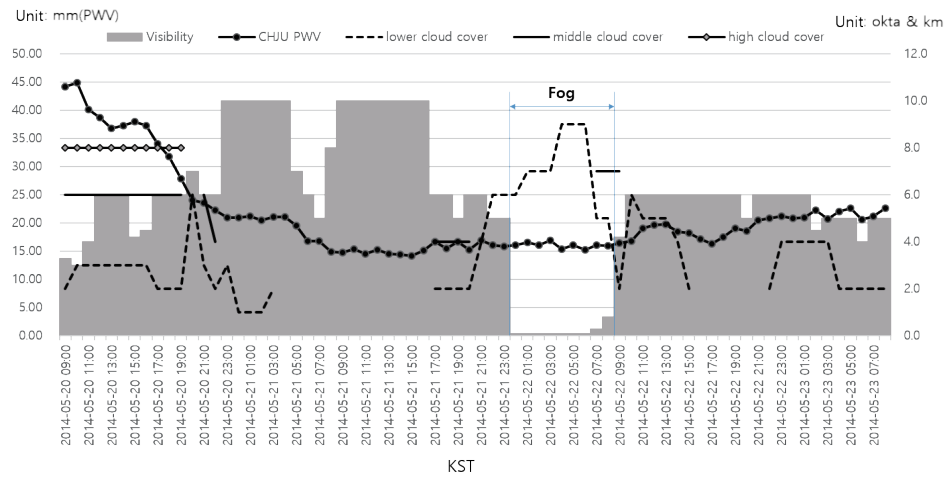
Fig. 13.   (Color online) Visibility and cloud coverage for different altitudes at Jeju Airport, and PWV of CHJU GNSS Station in May 2014.
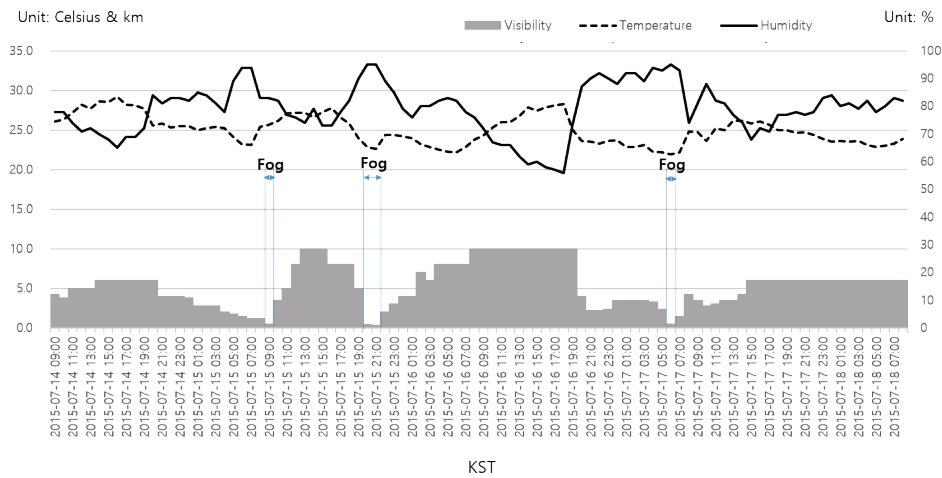
Fig. 14.   (Color online) Visibility, temperature, and humidity at Jeju Airport in July 2015.
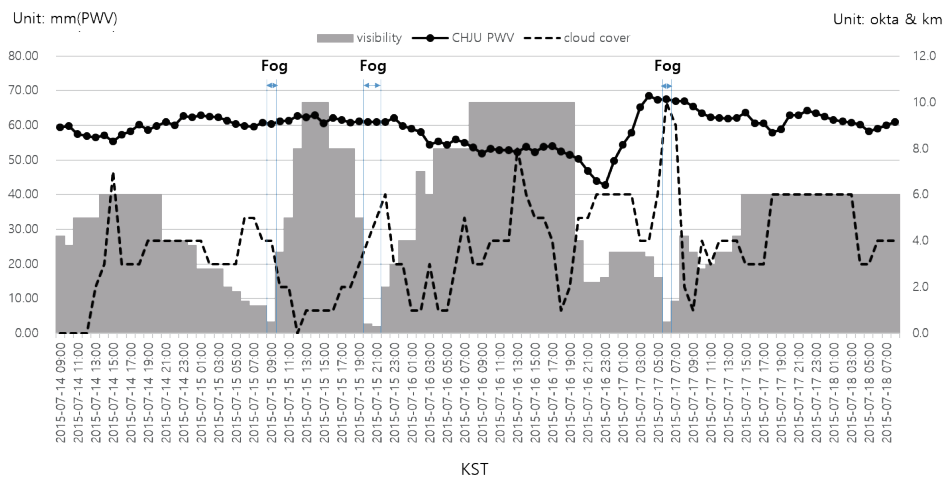
Fig. 15.   (Color online) Visibility and cloud coverage at Jeju Airport, and PWV of CHJU GNSS Station in July 2015.

There was a lot of rain from 7 to 12 July, but no precipitation from 14 to 18 July, when the fog occurred. However, the humidity remained high, the change in *PWV* was small, and *PWV* was high. For this reason, the correlation with cloudiness was low, unlike the other cases. The third period of foggy conditions occurred when *PWV* changed significantly, first increasing and then decreasing. At this time, middle-level clouds were observed (Fig. 16). In contrast, during the first and second foggy periods (15 July), low-level cloudiness increased, but there was no significant effect on *PWV*.

3.2.5   CASE 5: Fog analysis on 13–15 April 2016

In 2016, fog appeared from 20:00 on 12 April to 01:00 on 14 April, and again from 3:00 to 4:00 on 15 April (Fig. 17). Figure 18 shows the change in *PWV*. There was precipitation on 12 and 13 April and the changes in *PWV* were significant. When the fog appeared, there was a
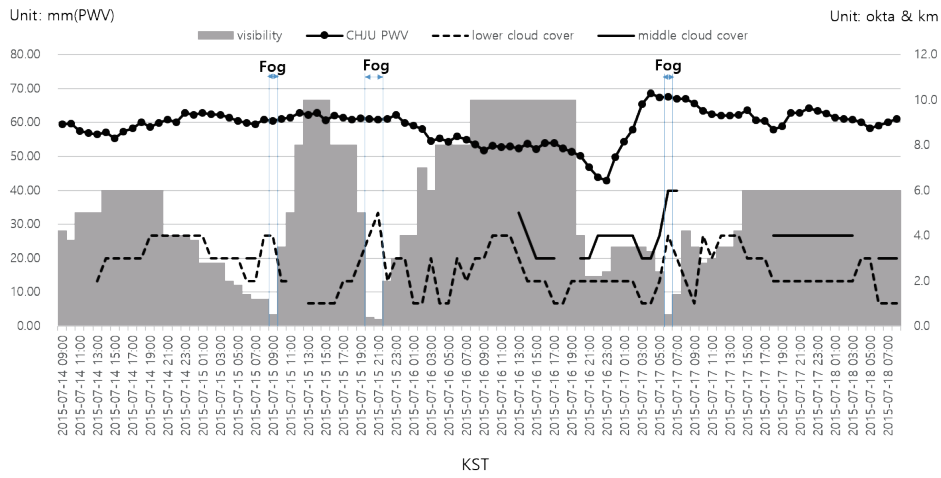
Fig. 16. (Color online) Visibility and cloud coverage for different altitudes at Jeju Airport, and PWV of CHJU GNSS Station in July 2015.
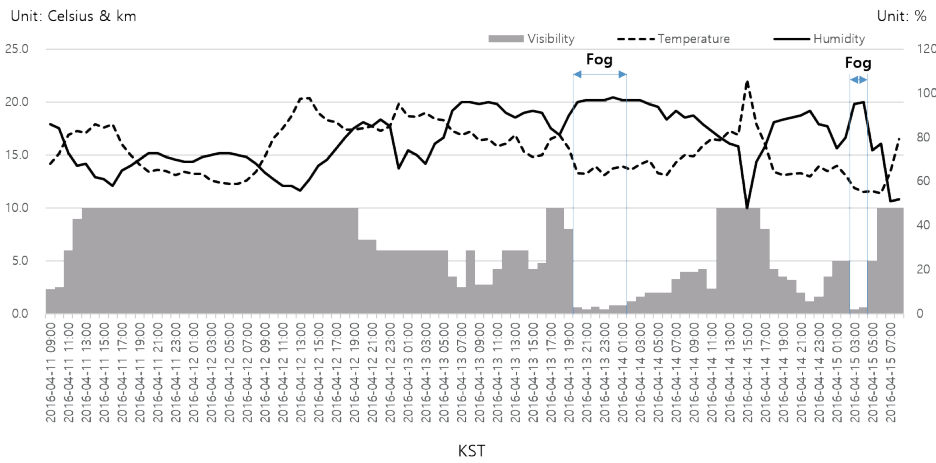
Fig. 17.   (Color online) Visibility, temperature, and humidity at Jeju Airport in April 2016.
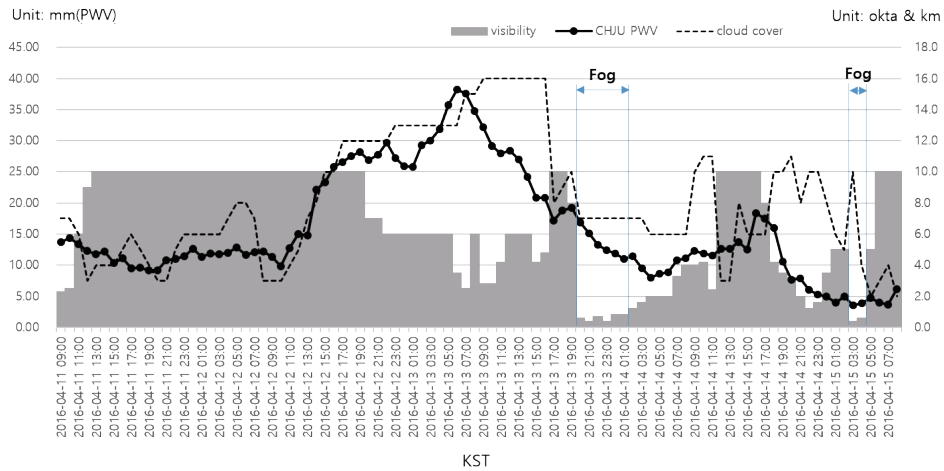
Fig. 18. (Color online) Visibility and cloud coverage at Jeju Airport, and PWV of CHJU GNSS Station in April 2016.

slight increase in *PWV* and then a decrease. This phenomenon occurred again, albeit weakly, during the second foggy period; in this case, the correlation between cloudiness and *PWV* was very high.

Figure 19 shows the cloudiness according to altitude level. As in the previous cases, it was found that the middle-level and high-level clouds, rather than the low-level clouds, affected the change in *PWV*.

3.2.6 Comprehensive analysis

In this study, we analyzed 20 fog cases from 2012 to 2016 at Jeju Airport; analysis results showed that the correlation between cloudiness and *PWV* was high (Tables 5 and 6). Positive correlations did not occur for all cases, but negative or low positive correlations occurred for the high humidity or low weighting of middle- and high-level cloudiness. This means that using GNSS *PWV* can also be a promising tool to detect cloudiness.
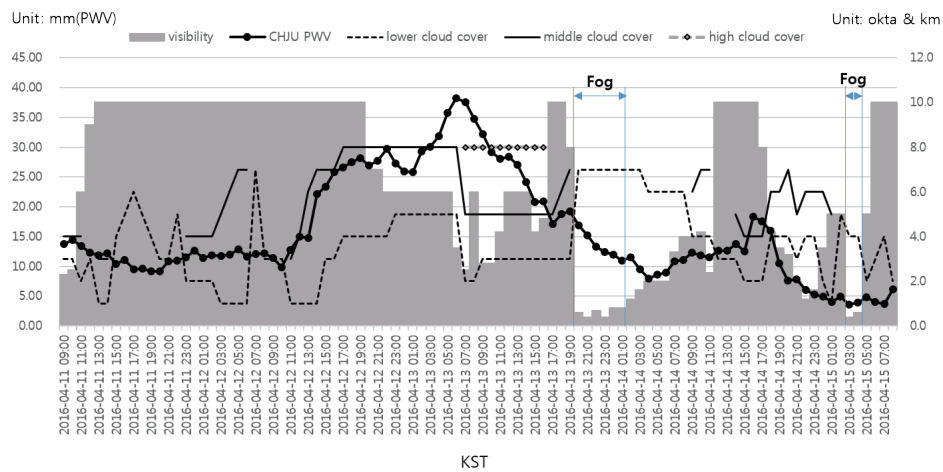
Fig. 19. (Color online) Visibility and cloud coverage for different altitudes at Jeju Airport, and PWV of CHJU GNSS Station in April 2016.

Table 5
Correlation between cloudiness and PWV.

Date	Correlation	Date	Correlation	Date	Correlation	Date	Correlation
28/03/12	0.894	04/05/12	0.839	05/09/12	−0.219	07/20/12	0.721
07/03/13	0.466	15/05/13	0.679	05/22/13	0.496	06/06/13	0.569
15/06/13	0.711	27/03/14	0.919	05/22/14	0.759	07/19/14	0.728
06/08/14	0.758	30/03/15	0.583	05/20/15	−0.217	07/16/15	−0.044
28/07/15	0.548	13/04/16	0.775	06/07/16	0.484	06/13/16	0.632

Table 6
Classifications of correlation.

Correlation	0.7–1.0	0.4–0.7	0–0.4	−0.3–0
Number	9	8	0	3

4. Conclusions

The analysis of changes in PWV during fog generation demonstrates that fog monitoring with PWV using GNSS is difficult and requires more precise GNSS processing. However, the relationship between cloudiness and PWV confirms that cloudiness affects changes in PWV. In particular, the change in PWV is affected by high-level and middle-level clouds. This appears to cause a delay in the GNSS signal, which must penetrate through more clouds. Many previous studies have analyzed GNSS PWV for rain or typhoons, but few have performed a comparison of GNSS PWV values with cloudiness on clear days, as performed here. The results of this study will aid in more quantitative cloudiness measurements, which at present are mostly performed through visual inspection. Furthermore, these results are expected to be helpful in the development of automatic observation devices for cloudiness measurements, satellite image processing, and weather forecasting.

Future research will focus on the tomography of the tropospheric delay in order to form a clearer understanding of the relationship between cloudiness and PWV. In addition, more meteorological elements and spatial topographic analysis should be added to monitor low-level clouds and fogs using GNSS.

Acknowledgments

References

1 Fog Compared with Mist: https://cloudatlas.wmo.int/en/fog-compared-with-mist.html (accessed July 2022).
2 M. Kunii, Y. Shoji, M. Ueno, and K. Saito: Meteorolog. Soc. Jpn. **88** (2010) 455. https://doi.org/10.2151/jmsj.2010-312
3 S. Shimizu, S. Shimada, and K. Tsuboki: J. Disaster Res. **12** (2017) 944. https://doi.org/10.20965/jdr.2017.p0944
4 Y. Shoji, M. Kunii, and K. Saito: Meteorolog. Soc. Jpn. **89** (2011) 67. https://doi.org/10.2151/jmsj.2011-105
5 J. Lee, J. Park, J. Cho, J. H. Baek, and H. W. Kim: Meteorol. Appl. **17** (2010) 463. https://doi.org/10.1002/met.182
6 A. Stoycheva and G. Guerova: Atmos. Sol. Terr. Phys. **133** (2015) 87. https://doi.org/10.1016/j.jastp.2015.08.004
7 A. Stoycheva, I. Manafov, K. Vassileva, and G. Guerova: Atmos. Sol. Terr. Phys. **161** (2017) 160. https://doi.org/10.1016/j.jastp.2017.06.011
8 M. Bevis, S. Businger, T. A. Herring, C. Rocken, A. R. Anthes, and H. R. Ware: Geophys. Res. D: Atmos. **97** (1992) 15787. https://doi.org/10.1029/92JD01517
9 J. Ha, K. D. Park, K. H. Chang, and H. Y. Yang: J. Korean Meteorol. Soc. **17** (2007) 291. https://www.koreascience.or.kr/article/JAKO200728839766153.page
10 J. Ha, K. D. Park, K. Kim, and Y. H. Kim: Asia-Pac. J. Atmos. Sci. **46** (2010) 233. https://doi.org/10.1007/s13143-010-1012-1
11 C. Park, J. Baek, and J. Cho: J. Astron. Space Sci. **26** (2009) 555. https://doi.org/10.5140/JASS.2009.26.4.555
12 C. Park, J. Cho, K. K. Shim, and B. C. Choi: Korean J. Remote Sens. **32** (2016) 263. https://doi.org/10.7780/kjrs.2016.32.3.6
13 T. Schuler: PhD Dissertation, Universitat der Bundeswehr, Munchen, Germany (2001). https://www.unibw.de/geodaesie/bau-9-1-ingenieurgeodaesie/downloads/dissertationen/heft-73.pdf
14 J. H. Baek, J. W. Lee, B. K. Choi, and J. H Cho: J. Astron. Space Sci. **24** (2007) 275. https://doi.org/10.5140/JASS.2007.24.4.275

15 G. Elgered, J. L. Davis, T. A. Herring, and I. I. Shapiro: J. Geophys. Res., Solid Earth **96** (1991) 6541. https://doi.org/10.1029/90JB00834

16 F. H. Webb and J. F. Zumberge: An Introduction to the GIPSY/OASIS-II. (JPL Publishing, California, 1993). https://www.semanticscholar.org/paper/An-Introduction-to-the-GIPSY%2FOASIS-II-Webb/751223ed2b002c77281323b7bc2ed3c88a5885d3

17 R. Dach, S. Lutz, P. Walser, and P. Fridez: Bernese GPS Software Version 5.2. (Astronomical Institute Publishing, Switzerland, 2015). http://www.bernese.unibe.ch/docs/DOCU52.pdf

18 J. F. Zumberge, M. B. Heflin, D. C. Jefferson, and M. M. Watkins: J. Geophys. Res., Solid Earth **102** (1997) 5005. https://doi.org/10.1029/96JB03860

19 H. E. Park, K. M. Roh, S. M. Yoo, B. K. Choi, J. K. Chung, and J. Cho: J. Position. Navig. Timing **3** (2014) 131. https://doi.org/10.11003/JPNT.2014.3.4.131

20 H. Park, S. Yoo, H. Yoon, J. Chung, and J. Cho: J. Position. Navig. Timing **5** (2016) 75. https://doi.org/10.11003/JPNT.2016.5.2.075

21 J. Kim and T. Bae: J. Korean Soc. Surv. Geodesy **33** (2015) 317. https://doi.org/10.7848/ksgpc.2015.33.4.317

22 Hydrometeors Consisting of a Suspension of Particles in the Atmosphere: https://cloudatlas.wmo.int/fog.html (accessed April 2022).

23 J. Lee, J. Cho, J. Baek, J. U. Park, and C. Park: J. Korean Meteorol. Soc. **18** (2008) 417. https://www.koreascience.or.kr/article/JAKO200828839767048.page

About the Authors

Lee Wonjong received his B.S. degree from Chungnam National University, Daejeon, in 2014 and his M.S. degree from the Department of Geoinformatics, University of Seoul, in 2017. Since 2017, he has been a Ph.D student at the University of Seoul. His current research interests include GNSS meteorology. (wonjong2@uos.ac.kr)

Choi Yunsoo received his Ph.D. degree from the Department of Civil Engineering, Sungkyunkwan University, in 1992. From 1991 to 2001, he was an associate professor at Hankyong University. Since 2001, he has been a professor at the University of Seoul, and since 2018, he has been the president of Hydrography Society Korea. His current research interests include geographic information and GNSS meteorology. (choiys@uos.ac.kr)

Yoon Hasu received his Ph.D. degree from the Department of Geoinformatics, University of Seoul, in 2015. From 2016 to 2018, he was with the Korea Astronomy and Space Science Institute. Since 2020, he has been a researcher at the National Geographic Information Institute. His current research interests include GNSS meteorology and ocean tide loading. (hasu9@korea.kr)